

Renormalization of the quasiparticle hopping integrals by spin interactions in layered copper oxides

L. Hozoi and S. Nishimoto

Max-Planck-Institut für Physik komplexer Systeme, Nöthnitzer Str. 38, 01187 Dresden, Germany

C. de Graaf

ICREA Research Professor at the Department of Physical and Inorganic Chemistry,
Universitat Rovira i Virgili, Marcel·lí Domingo s/n, 43007 Tarragona, Spain

(Dated: May 5, 2018)

Holes doped within the square CuO_2 network specific to the cuprate superconducting materials have oxygen $2p$ character. We investigate the basic properties of such oxygen holes by wavefunction-based quantum chemical calculations on large embedded clusters. We find that a $2p$ hole induces ferromagnetic correlations among the nearest-neighbor Cu $3d$ spins. When moving through the antiferromagnetic background the hole must bring along this spin polarization cloud at nearby Cu sites, which gives rise to a substantial reduction of the effective hopping parameters. Such interactions can explain the relatively low values inferred for the effective hoppings by fitting the angle-resolved photoemission data. The effect of the background antiferromagnetic couplings of renormalizing the effective nearest-neighbor hopping is also confirmed by density-matrix renormalization-group model Hamiltonian calculations for chains and ladders of CuO_4 plaquettes.

I. INTRODUCTION

Most theoretical models for high-temperature superconductivity are based on Hubbard or $t - J$ Hamiltonians with one orbital per CuO_4 plaquette. For the square lattice, the tight-binding part of such models reads in the \mathbf{k} representation $\epsilon(\mathbf{k}) = -2t(\cos k_x + \cos k_y) + 4t'\cos k_x \cos k_y - 2t''(\cos 2k_x + \cos 2k_y) + \dots$, where t is the hopping integral between nearest neighbors and t' and t'' are hoppings between second and third order neighbors. The values of these parameters were estimated by fitting the angle-resolved photoemission spectroscopy (ARPES) experimental data, see for example Refs. [1, 2, 3], and also by first principles investigations, both periodic density-functional calculations within the local density approximation (LDA) [4, 5, 6] and embedded cluster, wavefunction-based calculations [7, 8, 9]. The analysis of the LDA conduction bands in several copper oxide compounds yields a value of 0.4–0.5 eV for t and a ratio between the nearest-neighbor and next-nearest-neighbor hopping integrals $t'/t \approx 0.15$ for La_2CuO_4 [4, 6] and 0.33 for $\text{Tl}_2\text{Ba}_2\text{CuO}_6$ [6]. Wavefunction-based, quantum chemical calculations on finite clusters predict very similar nearest-neighbor hoppings, with t varying between 0.5 and 0.6 eV for different cuprate superconductors [7, 8, 9], with the observation that t corresponds in this case to the propagation of an oxygen $2p$ hole and not to d -like conduction-band states. However, these estimates are quite far from the numbers obtained by fitting the ARPES data. Such procedures give usually nearest-neighbor hopping integrals in the range of 0.10–0.30 eV for hole doping and 0.10–0.20 eV for the electron doped materials [1, 2, 3].

This paper presents a careful analysis of the characteristics of oxygen $2p$ holes doped into the spin-1/2 antiferromagnetic CuO_2 layer [10]. We perform *ab initio* multi-configuration calculations [11] on clusters that are large

enough to account for charge *and* spin relaxation and polarization effects in the near surrounding. We show that the hopping of the doped particle is strongly renormalized by spin interactions with and among the $S=1/2$ Cu d^9 neighbors and that by properly taking into account these effects, good agreement is found with the estimates extracted from the photoemission data for the hopping integrals. Our study is able to explain thus the difference between these “fitted” tight-binding parameters and the results of previous embedded cluster quantum chemical investigations or periodic density-functional calculations. The strong renormalization of the nearest-neighbor effective hopping found by *ab initio* wavefunction-based quantum chemical methods is confirmed by density-matrix renormalization-group (DMRG) [12, 13] model Hamiltonian calculations on chains and ladders of CuO_4 plaquettes.

II. CHARGE AND SPIN CONFIGURATION AROUND A DOPED HOLE

To illustrate the nature of an oxygen hole in the CuO_2 plane, we first discuss results of multiconfiguration self consistent field (MCSCF) calculations on a 9-plaquette square cluster, see Fig.1. This cluster includes nine Cu ions and twenty four in-plane oxygens but no apex ligands. The geometrical structure corresponds to that of the hole doped $\text{La}_{1.85}\text{Sr}_{1.85}\text{CuO}_4$ compound [14]. We use effective core potentials (ECPs) for the $1s, \dots, 3s$ inner shells of each transition metal center and the $1s$ core of the oxygens at the boundaries of the cluster, as developed by Seijo *et al.* [15] and Bergner *et al.* [16], respectively. For the outer shells of these ions we apply the following gaussian-type basis sets: Cu ($9s6p6d$)/[$3s3p3d$] [15] and O ($4s5p$)/[$2s3p$] [16]. Still, the rest of the ligands, i.e. those bridging the cluster Cu ions (see Fig.1(a)), are rep-

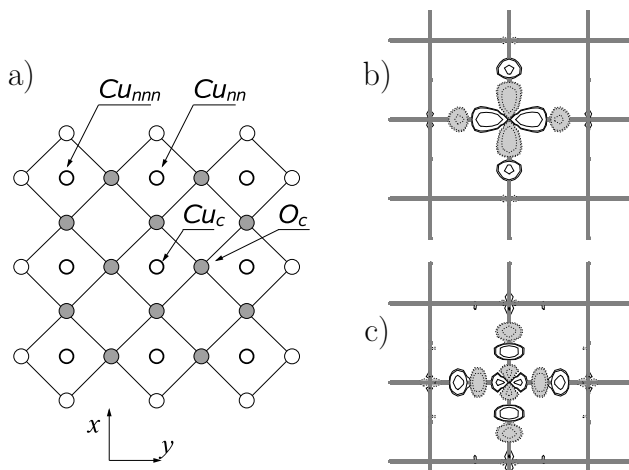


FIG. 1: (a) The 9-plaquette $[\text{Cu}_9\text{O}_{24}]$ cluster employed for studying the distribution of an O $2p$ hole. O ions that are modeled with all-electron basis sets are shown in grey. (b)-(c) B and AB pd orbitals defining the ZR-like state on the central Cu_cO_4 plaquette. Their occupation numbers are 1.80 and 0.20. Positive and negative lobes of the p and d functions are shown in white and gray, respectively. For the B combination the p and d AOs are strongly overlapping.

resented with all-electron basis sets with a $(14s9p)/[4s3p]$ contraction scheme [17]. Our clusters are always embedded in large arrays of point charges at the experimental lattice positions that reproduce the crystal Madelung field. The Cu^{2+} and La^{3+} nearby neighbors are represented by total ion potentials [18]. The calculations were performed with the MOLCAS 6 program package [19].

Multiconfiguration, complete active space (CAS) [11] calculations were carried out for a single hole “doped” into the 9-plaquette cluster. We employed a minimal CAS for constructing the multiconfiguration wavefunction, with ten electrons distributed in all possible ways over ten active orbitals. Those are the nine $\text{Cu } 3d_{x^2-y^2}$ orbitals plus one O $2p$ orbital. The rest of the Cu $3d$ and O $2p$ orbitals and the other lower-energy orbitals are doubly occupied in all configurations and do not participate to the construction of the MC expansion. The ground-state has overall singlet spin multiplicity and corresponds to the formation of a pd Zhang-Rice (ZR) [20] -like configuration on the central Cu_cO_4 plaquette. Mulliken charge and spin populations, MCPs and MSPs, respectively, are collected for this state in Table I. The bonding (B) and antibonding (AB) pd ZR orbitals are plotted in Fig.1(b-c). Their occupation numbers are 1.80 and 0.20, respectively. The Mulliken charges of the oxygen $2p_x$ and $2p_y$ atomic orbitals (AOs) forming the pd B and AB combinations on the ZR plaquette are similar to the values reported in [21, 22]. The Mulliken charges associated with the Cu $3d_{x^2-y^2}$ functions are slightly larger due to the different basis sets employed here.

The formation of CuO_4 pd singlet states as predicted by Zhang and Rice [20] was previously confirmed by the *ab initio* study of Calzado and Malrieu [7, 8]. Two of us

investigated in Refs. [21, 22] electron-lattice interactions associated with such configurations. It was found that the ZR state is stabilized by lattice relaxation effects involving a shortening by few percents of the Cu–O bonds. The magnitude of the stabilization energy indicates that the doped holes form small polarons in cuprates, at least at low concentrations. In this paper, however, we are mainly concerned with pure electronic effects, that determine the characteristics of the ZR-like quasiparticle. All calculations are therefore performed on high-symmetry, undistorted clusters using the average Cu–O distances reported in Ref. [14]. For the $[\text{Cu}_9\text{O}_{24}]$ square cluster depicted in Fig.1, both ZR-like states and broken-symmetry solutions with the $2p$ hole having the largest weight at a single oxygen site were obtained. Such O $2p^5$ -like states were discussed in Ref. [21]. The energy difference between the ZR Cu_cO_4 state and a broken-symmetry O_c $2p^5$ -like state is 5 meV in the $[\text{Cu}_9\text{O}_{24}]$ cluster, with the ZR configuration lower in energy. The broken-symmetry configurations may be favored, however, by inter-carrier Coulomb and spin interactions. Effects of such interactions between two or more holes were investigated in Ref. [23] by calculations on 7-plaquette linear clusters. For an undistorted 7-plaquette cluster and a single doped hole, the energy difference between the ZR state and a broken-symmetry $2p^5$ -like state, both involving oxygens ions on the same plaquette, is again very small, about 5 meV, but the order of the states is reversed. This different ordering of the states is due to finite-size effects in the linear cluster [24]. To conclude this part of our discussion, the calculations on the large 9-plaquette cluster show that an isolated O $2p$ hole, i.e. an oxygen hole at sufficiently low doping, should be viewed as part of a pd ZR-like state even if the local lattice relaxation effects are neglected. Our estimation of the nearest-neighbor and next-nearest-neighbor hopping matrix elements will be based on such a ZR-like quasiparticle picture.

A distinctive feature of the results listed in Table I is the nature of some of the spin couplings. The spin populations given in the last column are obtained from the difference between the “up” and “down” spin densities. The very low values associated with the Cu $d_{x^2-y^2}$ and O p_x and p_y orbitals forming the linear combinations de-

TABLE I: Mulliken population analysis illustrating the distribution of an O $2p$ hole and the nature of the Cu–Cu spin couplings, see text. CASSCF results for a 9-plaquette cluster. Notations as in Fig.1 are used. For each of the O_c , Cu_{nn} , and Cu_{nnn} ions, there are another three equivalent sites.

Relevant AOs	MCPs	MSPs
$\text{Cu}_c 3d_{x^2-y^2}$	1.17	0.06
$\text{O}_c^{x,y} 2p_{x,y}$	1.62 ^a	−0.01
$\text{Cu}_{nn}^{x,y} 3d_{x^2-y^2}$	1.27	0.31
$\text{Cu}_{nnn}^{x,y} 3d_{x^2-y^2}$	1.28	−0.32

^aThe Mulliken charges of the other in-plane oxygen atomic orbitals are not smaller than 1.8.

TABLE II: Nearest-neighbor hopping integrals as obtained by CASSCF/CASSI calculations on clusters of different sizes, see text. Mulliken charge populations for the O $2p$ AOs forming the σ $p_{x,y}-d_{x^2-y^2}$ bonds on a ZR plaquette are also listed.

Cluster	t (eV)	O-hole AOs, MCPs:		
		p_y ,	p'_y ,	p_x
[Cu ₆ O ₁₉] ^a	0.310	1.61, 1.61,	1.60	
[Cu ₆ O ₁₇] ^b	0.165	1.61, 1.63,	1.63	
	0.160	1.60, 1.64,	1.63	
[Cu ₁₀ O ₂₉] ^c	0.135	1.65, 1.61,	1.63	

^aLinear cluster, all-electron (AE) basis sets (BSs) [28].

^b3 by 2 plaquettes, see text. Results with AE BSs, first line, and with ECPs for the ions outside the active region, next line.

^cECPs were used for part of the Cu and O ions, see text.

picted in Fig.1(b-c) indicate indeed that the dominant contribution to the many-electron wavefunction comes from configurations where the d and p holes on the Cu_cO₄ plaquette are coupled to a singlet. The fact that these numbers are not exactly zero shows that configurations related to different and more complicated spin coupling schemes, involving also adjacent d spins, contribute to the MC wavefunction too. Such $d-p-d$ interactions in the presence of the oxygen hole induce actually ferromagnetic spin correlations between the $d_{x^2-y^2}$ electron at the “central” Cu_c site and the nearest-neighbor $d_{x^2-y^2}$ electrons, as illustrated by the Mulliken spin populations listed in Table I.

The dressing of an O hole by a two-dimensional ferromagnetic spin polarization cloud was previously suggested by Hizhnyakov and Sigmund [25] on the basis of Hubbard-like pd model Hamiltonian calculations. Nevertheless, the dominant interactions are those between the d and p electron holes on a single CuO₄ plaquette such that this object may be viewed as a ZR-like quasiparticle. As expected, the data from Table I also show that farther $d-d$ interactions, between first and second order Cu neighbors to the central plaquette are antiferromagnetic.

III. RENORMALIZATION OF THE HOPPING INTEGRALS BY SPIN INTERACTIONS

The effect of spin interactions on the nearest-neighbor and next-nearest-neighbor hopping integrals can be evaluated by calculations on clusters of different sizes, where the O-mediated $d-d$ magnetic couplings are included either for all or only part of the transition metal neighbors. For clusters that are large enough, we can take into account both the ferromagnetic correlations between the d electron on the ZR plaquette and its nearest neighbors and the effect of the background antiferromagnetic couplings.

The clusters we employ for our investigation always include a 2-plaquette “active” region with one oxygen $2p$ hole plus a variable number of neighboring (undoped)

plaquettes. The copper and oxygen ions on the two “active” plaquettes are modeled by all-electron split-valence basis sets of triple-zeta quality [28]. Depending on the size of the cluster, for the other cluster ions we either apply the same all-electron basis sets or use effective potentials for the core electrons. As mentioned above, point charges and total ion potentials are used for representing the rest of the crystal. For each cluster, we first determine the two equivalent CASSCF solutions where the $2p$ hole is localized either on the “left” or on the “right” plaquette of the active region. Since these states are obtained by separate SCF calculations, they are non-orthogonal and interacting. Non-interacting, orthogonal eigenstates can be obtained by State Interaction (SI, or CASSI) calculations [30]. The effective hopping integral is half of the energy separation between these CASSI eigenstates [31]. In terms of matrix elements between the separately optimized CASSCF wavefunctions, it can be written as $t_{\text{eff}} = (H_{ij} - S_{ij}H_{ii})/(1 - S_{ij}^2)$, where H_{ij} and S_{ij} denote Hamiltonian and overlap matrix elements between N -electron states i and j , respectively.

For all calculations we use a minimal active space, with one active orbital for each d and p hole. The total spin multiplicity is doublet because we always consider an even number of plaquettes (or Cu sites) and a single doped hole. During the CASSCF optimization for a particular $2p$ -hole quasilocized state not only the electronic charge is allowed to relax but also the spin configuration of the nearby Cu $d_{x^2-y^2}$ electrons is let to readjust, see for example the discussion in Refs. [32, 33, 34, 35]. Our approach for estimating the effective hoppings resembles in fact an idea proposed earlier by Eder and Becker [36], of setting up an effective tight-binding Hamiltonian $H_{\text{eff}} = \sum_{ij} t_{\text{eff}} (c_i^\dagger c_j + h.c.)$, where c_i^\dagger and c_i consist of a sum of products of a “bare” fermion operator and a number of spin flip operators. We note that for each hopping process within a “rigid” Néel lattice the energy of the system increases by $3J/2$ [35]. This quantity, about 0.2 eV (the value of the antiferromagnetic coupling constant is 120–140 meV [37]), is comparable with the bare nearest-neighbor hopping of 0.4–0.5 eV, see Refs. [4, 5, 6, 7, 8, 9] and the results discussed below. By considering also the spin polarization effect described in the previous section, it can be argued that the magnetic energy associated with the disordered spins created at each hopping [35] has the same magnitude with the bare hopping integral, i.e. the hopping of the $2p$ hole and the spin relaxation in the immediate vicinity imply similar time scales. Our procedure of mapping the *ab initio* data onto an effective tight-binding Hamiltonian including also spin relaxation effects is thus justified.

pd ZR-like solutions where the oxygen hole is equally distributed over the four ligands of a given plaquette could not be obtained for 2-plaquette and linear 4-plaquette clusters with no distortions. For such clusters, the O hole has always the largest weight onto one of the ligands connecting two Cu ions. The smallest linear cluster where the CASSCF calculations converge to

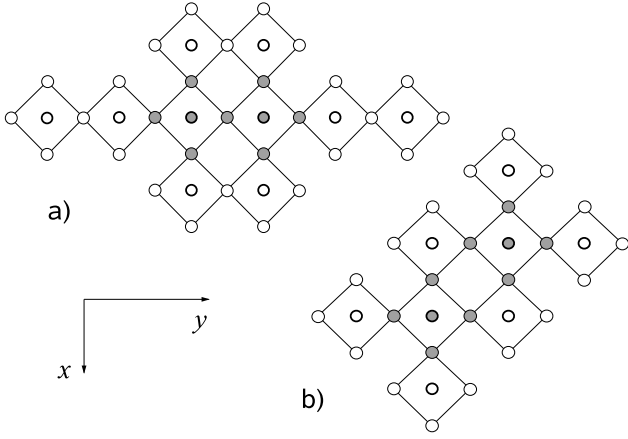


FIG. 2: (a) Sketch of the 10-plaquette $[\text{Cu}_{10}\text{O}_{29}]$ cluster used for evaluating the nearest-neighbor hopping t . The ions in the “active” region are shown in grey. The 6-plaquette $[\text{Cu}_6\text{O}_{17}]$ cluster is obtained by removing the four plaquettes on the same axis with the Cu ions of the active region. (b) The 8-plaquette $[\text{Cu}_8\text{O}_{24}]$ atomic configuration used for evaluating t' .

symmetric pd ZR-like solutions is a 6-plaquette cluster. Results obtained by CASSCF and CASSI calculations on the 6-plaquette linear cluster are shown on the first line of Table II. All-electron basis sets were applied in this case for each ion of the cluster [28].

The minimal-CAS SI nearest-neighbor hopping for the 6-plaquette linear cluster is 0.310 eV. This value decreases dramatically, however, when the cluster is enlarged such that it includes the other four CuO_4 plaquettes which are first order neighbors of the two active plaquettes. This is a 10-plaquette cluster, schematically drawn in Fig. 2(a). In order to reduce the computational effort we used again, as in the 9-plaquette square cluster, the ECPs of Seijo *et al.* [15] and Bergner *et al.* [16] for the copper and oxygen ions outside the active region, with the following basis sets for the Cu $3p, 3d, 4s, 4p$ and O $2s, 2p$ outer shells: Cu $(9s6p6d)/[3s2p2d]$ and O $(4s5p)/[2s3p]$. The CASSCF/SI estimate of the nearest-neighbor hopping integral for the 10-plaquette cluster is given on the last line of Table II. This value, 0.135 eV, is less than half of the estimate for the 6-plaquette linear cluster. As mentioned above, both charge and spin relaxation are allowed during the SCF optimization. The Mulliken spin populations for the CASSCF solution with the O hole localized on the left-hand plaquette of the active region are displayed in Fig. 3. It can be easily noticed that the symmetry equivalent CASSCF ZR-like solution with the O hole on the right-hand plaquette implies some rearrangements for the spin configuration at the neighboring Cu sites.

CASSCF and CASSI calculations were also carried out on a 6-plaquette cluster obtained by removing from the 10-plaquette cluster those four plaquettes on the same axis with the copper ions of the active region, see Fig. 2(a). The nearest-neighbor hopping matrix el-

ement is approximately 0.17 eV in this case, see Table II. This value is again much lower than the number extracted from the linear cluster. Still, since spin interactions are taken into account for only part of the nearest-neighbor plaquettes around the ZR-like quasiparticle, it is larger than the estimate for the 10-plaquette cluster. It is worthwhile noting that the value of this parameter changes only little when using effective core potentials instead of all-electron basis sets for the ions outside the active region, see the results for the $[\text{Cu}_6\text{O}_{17}]$ cluster in Table II. We also point out that the occupation numbers of the σ $p-d$ B and AB combinations on the ZR plaquettes and the Mulliken charge populations of the $2p$ atomic orbitals accommodating the oxygen hole are very similar for all the Cu-O clusters discussed here. For comparison, Mulliken charge populations are listed in both Table I and Table II. Due to the symmetry properties of the atomic configurations given in Table II and Fig. 2(a), the p_y ZR-like orbitals on a CuO_4 plaquette are not equivalent, and we denote these orbitals as p_y and p'_y , where p_y connects the two Cu sites of the active region.

A different numerical experiment that confirms the effects illustrated in Table II is to replace the eight $\text{Cu}^{2+} 3d^9$ cations surrounding the two active plaquettes in the 10-plaquette cluster, see Fig. 2(a), with closed-shell $\text{Zn}^{2+} 3d^{10}$ ions [38]. The CASSI estimate for t in this $[\text{Cu}_2\text{Zn}_8\text{O}_{29}]$ cluster is 0.450 eV, larger than all values listed in Table II. For a $[\text{Cu}_6\text{Zn}_4\text{O}_{29}]$ atomic configuration where only those four Cu neighbors are replaced by $\text{Zn}^{2+} 3d^{10}$ ions which are not situated along the same line with the “active” Cu sites, t is lowered to 0.330 eV, close to the estimate in the linear $[\text{Cu}_6\text{O}_{19}]$ cluster from Table II. This latter value is about two times larger than in the $[\text{Cu}_{10}\text{O}_{29}]$ cluster and indicates that the effect of

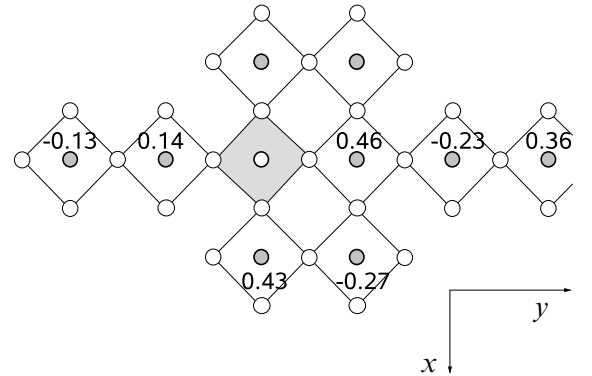


FIG. 3: CASSCF Mulliken d -spin populations for a 10-plaquette cluster with one O hole. The ZR-like plaquette is represented with a filled square. The MSPs for the Cu and each O ion on this plaquette are 0.07 and -0.01 , respectively. The equivalent CASSCF state used to calculate the effective nearest-neighbor hopping can be obtained by a reflection through one of the symmetry planes of the cluster. For the two CASSCF ZR-like states, different spin populations are associated with the nearby Cu sites.

interactions with and among Cu d spins which are not located along the direction of propagation is stronger than the effect of the collinear spin interactions.

The next-nearest-neighbor hopping, usually denoted as t' , was evaluated by calculations on an 8-plaquette cluster like that sketched in Fig.2(b). We applied the same ECP basis sets as for the 10-plaquette cluster for the O and Cu ions surrounding the 2-plaquette active region, see above. All-electron basis sets were employed for the ligands in the active region [28], but the two active cations were also modeled with ECPs [15]. The following basis sets were applied for the $3p, 3d, 4s, 4p$ shells at these transition metal sites: Cu ($9s6p6d/[3s3p3d]$) [15]. Our CASSI estimate for t' is 0.015 eV, which gives a t'/t ratio of 0.11 in the weakly doped La_2CuO_4 system. A ratio $t'/t = 0.12$ was obtained by fitting the ARPES data for an overdoped $\text{La}_{2-x}\text{Sr}_x\text{CuO}_4$ sample [39] and $t'/t = 0.24$ for $\text{Bi}_2\text{Sr}_2\text{CaCu}_2\text{O}_8$ [1].

A few words are in place concerning the comparison between our present results and the results of other *ab initio* wavefunction-based investigations for copper oxide superconductors. A first issue is related to the nature of the active orbital space employed for the multiconfiguration calculations. For the 2-plaquette “active” cluster region we always consider a CAS with three electrons and three orbitals. These three orbitals are a bonding $p-d$ linear combination, an essentially nonbonding d (or $d-d$) component, and an antibonding $p-d$ orbital. The bonding $p-d$ combination is usually [8, 9] included in the inactive, doubly occupied orbital set, which gives an active space with one electron and two orbitals if other d orbitals around the 2-plaquette active cluster region are omitted. However, the occupation numbers associated with the pair of $p-d$ bonding and antibonding orbitals in the 3-orbital CAS, about 1.8 and 0.2, respectively (see the discussion above and Fig.1(b-c)), indicate significant non-dynamical correlation effects [11]. As a zeroth-order approximation, the 3-orbital CAS seems to be then more appropriate for studying the character and the properties of a doped hole. Multi-reference, difference-dedicated configuration interaction (DDCI) [40] calculations with reference wavefunctions having either two or three orbitals in the active space were performed on a hole doped 2-plaquette cluster by Calzado and Malrieu [7]. They found that in the 2-plaquette cluster the DDCI estimate for the nearest-neighbor hopping is in fact quite insensitive to the size of the active orbital space. In addition, an iterative DDCI (IDDCI) scheme [41] was applied in Ref. [7] for generating average molecular orbitals and to obtain an unbiased representation of the two states used to extract t . It was concluded that the description of the oxygen hole in the IDDCI wavefunction is only little affected when decreasing the size of the active space from three to two orbitals.

For a 2-plaquette $[\text{Cu}_2\text{O}_7]$ cluster and all-electron basis sets [28] our CASSI estimate for the nearest-neighbor hopping integral is 0.650 eV, rather similar to the IDDCI value reported in Ref. [7], $t = 0.575$ eV [42]. As already

mentioned above, the “left” and “right” -localized O hole states are asymmetric in the 2-plaquette cluster. Using the same notations as in Table II, the Mulliken charge populations of the p_y , p'_y , and p_x orbitals are 1.32, 1.74, and 1.68, respectively.

A straight comparison between our CASSCF/SI results and the DDCI/IDDCI data of Calzado and Malrieu is not possible. It is known [7, 43, 44], however, that DDCI/IDDCI brings rather small corrections to the CASCI/CASSCF estimates for the nearest-neighbor hoppings on 2-plaquette clusters in various cuprates, not larger than 15% [43, 44]. This suggests that dynamical electron correlation is not essential in determining the magnitude of the hopping integrals, as already pointed out in Refs. [43, 44], for example. In any case, the *spin* polarization and relaxation effects at adjacent Cu sites evidenced by our calculations on clusters of different sizes are mainly related to non-dynamical electron correlation, and induce changes of the hopping parameter about an order of magnitude larger than the corrections brought by DDCI in 2-plaquette clusters. We also note that with the CASSCF/SI approach we are able to treat explicitly *charge* relaxation and polarization due to the creation of an oxygen hole on a given CuO_4 plaquette. In the context of *ab initio* calculations for estimating effective electronic-structure parameters such effects are sometimes referred to as dynamical repolarization effects. That a compact, transparent, and rather accurate description is obtained when the most important configurations contributing to the many-electron wavefunction are expressed in terms of individually optimized orbital sets was previously shown for the calculation of magnetic exchange coupling constants [45] and core-level photoionized states [46] in transition metal oxides.

An effective nearest-neighbor hopping parameter t can also be obtained by mapping the low-energy electronic states of the one-band Hubbard model onto those of a pd model. The pd Hamiltonian is given by the following expression:

$$\begin{aligned} H = & - t_{pd} \sum_{\langle ij \rangle \sigma} \left(d_{i\sigma}^\dagger p_{j\sigma} + p_{j\sigma}^\dagger d_{i\sigma} \right) \\ & - t_{pp} \sum_{\langle jl \rangle \sigma} \left(p_{j\sigma}^\dagger p_{l\sigma} + p_{l\sigma}^\dagger p_{j\sigma} \right) \\ & + \epsilon_d \sum_{i\sigma} d_{i\sigma}^\dagger d_{i\sigma} + \epsilon_p \sum_{j\sigma} p_{j\sigma}^\dagger p_{j\sigma} \\ & + U_d \sum_i d_{i\uparrow}^\dagger d_{i\uparrow} d_{i\downarrow}^\dagger d_{i\downarrow} + U_p \sum_j p_{j\uparrow}^\dagger p_{j\uparrow} p_{j\downarrow}^\dagger p_{j\downarrow} . \end{aligned}$$

t_{pd} is here the hopping matrix element between p and d orbitals at nearest-neighbor ligand and metal sites and the first sum is over all pairs of such nearest neighbors. It is assumed that t_{pd} takes the same value for all these Cu–O pairs. The second sum in the expression above is over all pairs of nearest-neighbor anions and t_{pp} is the corresponding matrix element. We have chosen the phases of the orbitals such that the sign of each of the two hopping

matrix elements is constant. The difference between the on-site d and p orbital energies is in the electron representation $\Delta_{pd} = \epsilon_d - \epsilon_p > 0$ and $U_d > 0$, $U_p > 0$ are the on-site Coulomb repulsion energies for Cu and O, respectively. For the parameters of our pd model we use typical values such as $t_{pd} = 1.5$, $t_{pp} = -0.8$, $\Delta_{pd} = 3$, $U_d = 8$, and $U_p = 4$, in units of eV. The effective one-band Hubbard model is given by

$$H = -t \sum_{\langle ij \rangle \sigma} (c_{i\sigma}^\dagger c_{j\sigma} + c_{j\sigma}^\dagger c_{i\sigma}) + U \sum_i c_{i\uparrow}^\dagger c_{i\uparrow} c_{i\downarrow}^\dagger c_{i\downarrow}.$$

t corresponds here to the effective hopping of the ZR-like quasiparticle between nearest-neighbor CuO_4 plaquettes. $U > 0$ is the “on-site” Coulomb interaction and we choose $U = 5$ eV.

Ground-state and excited-state calculations for the pd and the one-band Hubbard models are performed by using DMRG techniques. For hole-doped clusters of 6×1 and 6×3 CuO_4 plaquettes we found that the lowest-lying states in the two models have the same quantum numbers and the same character. We can make thus between the two models a simple one-to-one correspondence for several low-energy states. The effective hopping parameter t is then determined such that it minimizes a function

$$\delta E = \sum_{n=1}^4 (\Delta E_n^{pd} - \Delta E_n^{\text{Hub}})^2,$$

where $\Delta E_n^{pd} = E_n^{pd} - E_0^{pd}$ ($\Delta E_n^{\text{Hub}} = E_n^{\text{Hub}} - E_0^{\text{Hub}}$) are relative energies of the lowest four excited eigenstates in the pd (Hubbard) model. The ground-state is denoted with $n=0$. For 6×1 and 6×3 clusters, each doped with two holes, our mapping procedure gives effective t values of 0.51 and 0.28 eV, respectively. This reduction of t is due not only to the inclusion of antiferromagnetic correlations on the adjacent chains but also to an increase of the nearest-neighbor spin correlations along the chain. Within the pd model, the nearest-neighbor spin correlation function changes from -0.103 in the 6×1 chain to -0.152 for the central chain in the 6×3 ladder. For more chains this quantity is only slightly modified, to -0.158 for example in a 6×5 cluster. The model-Hamiltonian calculations confirm thus the renormalization effect found by *ab initio* quantum chemical methods. If six holes are doped into the 6×3 cluster, i.e. the hole concentration is kept constant with respect to the 6×1 2-hole configuration, the effective hopping is 0.29 eV, which shows that for this range of hole concentrations the doping dependence is very small.

IV. CONCLUSIONS

The interplay among charge, spin, and lattice degrees of freedom and the formation of composite spin-lattice polarons were studied in cuprates (and other transition metal oxide compounds) by many authors. In layered copper oxides, the spin mechanism responsible for polaronic-like behavior is associated with the fact that a charge carrier hopping to an adjacent site must disrupt, at least at relatively low doping, the antiferromagnetic spin configuration in its vicinity. Such effects were investigated by calculations based on one-band Hubbard and t - J models, see for example Refs. [47, 48, 49, 50, 51, 52]. These studies show indeed that the background antiferromagnetic correlations lead to band narrowing and a strong enhancement of the electron-phonon couplings. We are able to provide here *ab initio* numerical estimates for the effect of such interactions on the effective hopping integrals. The results can explain the relatively low values deduced for the quasiparticle hopping parameters from fits of the photoemission data.

Our *ab initio* calculations also show that an oxygen hole induces ferromagnetic correlations between the d electron on the ZR-like plaquette and the nearest-neighbor Cu d spins. Such effects are missing in one-band Hubbard or t - J models. At this moment we are not able to quantify the strength of these ferromagnetic interactions in the form of effective magnetic coupling constants or spin correlation functions, at least not at the *ab initio* level. Nevertheless, this spin polarization effect is one of the factors that determines the characteristics of the hole motion. It might also offer an explanation for the disappearance of long-range antiferromagnetic order at doping levels which are much lower as compared to the electron doped cuprates. It is interesting that for an isolated chain of plaquettes, “local” ferromagnetic correlations in the direction of propagation would tend to facilitate the motion of the hole, although the fact that the carrier perturbs the magnetic couplings beyond nearest neighbors results in a stronger and opposite effect. In addition to that, the effective hopping parameter depends strongly on interactions involving spins on adjacent chains, i.e. Cu d spins which are not situated along the direction of propagation of the hole. Qualitatively, this is also confirmed by mapping the solutions of a pd model Hamiltonian onto those of an effective one-band Hubbard model for clusters consisting of chains or ladders of plaquettes. The inclusion of the adjacent antiferromagnetic chains in a three-leg ladder determines a reduction of the effective nearest-neighbor hopping of about fifty percent in comparison to the case of a single chain.

-
- [1] M. R. Norman, Phys. Rev. B **61**, 14751 (2000).
 [2] M. C. Schabel, C.-H. Park, A. Matsuura, Z.-X. Shen, D.

A. Bonn, R. Liang, and W. N. Hardy, Phys. Rev. B **57**, 6090 (1998).

- [3] D. Manske, I. Eremin, and K. Bennemann, *Europhys. Lett.* **53**, 371 (2001).
- [4] M. S. Hybertsen, E. B. Stechel, M. Schluter, and D. R. Jennison, *Phys. Rev. B* **41**, 11068 (1990).
- [5] O. K. Andersen, A. I. Liechtenstein, O. Jepsen, and F. Paulsen, *J. Phys. Chem. Solids* **56**, 1573 (1995).
- [6] E. Pavarini, I. Dasgupta, T. Saha-Dasgupta, O. Jepsen, and O. K. Andersen, *Phys. Rev. Lett.* **87**, 047003 (2001).
- [7] C. J. Calzado and J.-P. Malrieu, *J. Chem. Phys.* **112**, 5158 (2000).
- [8] C. J. Calzado and J.-P. Malrieu, *Phys. Rev. B* **63**, 214520 (2001).
- [9] D. Muñoz, I. de P. R. Moreira, and F. Illas, *Phys. Rev. B* **65**, 224521 (2002).
- [10] The undoped configuration implies Cu $3d^9$ and O $2p^6$ formal valence states (each O $2p$ orbital is doubly occupied).
- [11] For a monograph, see T. Helgaker, P. Jørgensen, and J. Olsen, *Molecular Electronic-Structure Theory* (Wiley, Chichester, 2000).
- [12] S. R. White, *Phys. Rev. B* **48**, 10345 (1993).
- [13] For a review, see U. Schollwöck, *Rev. Mod. Phys.* **77**, 259 (2005).
- [14] R. J. Cava, A. Santoro, D. W. Johnson, and W. W. Rhodes, *Phys. Rev. B* **35**, 6716 (1987).
- [15] L. Seijo, Z. Barandíaran, and S. Huzinaga, *J. Chem. Phys.* **91**, 7011 (1989).
- [16] A. Bergner, M. Dolg, W. Küchle, H. Stoll, and H. Preuss, *Mol. Phys.* **80**, 1431 (1993).
- [17] P.-O. Widmark, P.-Å. Malmqvist, and B. O. Roos, *Theor. Chim. Acta* **77**, 291 (1990).
- [18] F. Illas, J. Rubio, J. C. Barthelat, *Chem. Phys. Lett.* **119**, 397 (1985); W. R. Wadt and P. J. Hay, *J. Chem. Phys.* **82**, 284 (1985).
- [19] MOLCAS 6, Department of Theoretical Chemistry, University of Lund, Sweden.
- [20] F. C. Zhang and T. M. Rice, *Phys. Rev. B* **37**, 3759 (1988).
- [21] L. Hozoi, S. Nishimoto, and A. Yamasaki, *Phys. Rev. B* **72**, 144510 (2005).
- [22] L. Hozoi and S. Nishimoto, *Phys. Rev. B* **73**, 245101 (2006).
- [23] L. Hozoi, S. Nishimoto, G. Kalosakas, D. B. Bodea, and S. Burdin, cond-mat/0605578 (unpublished).
- [24] Finite-size effects are also responsible for a different order of these states in the case of CASSCF calculations on a $[\text{Cu}_5\text{O}_{26}]$ square cluster in Ref. [21].
- [25] V. Hizhnyakov and E. Sigmund, *Physica C* **156**, 655 (1988); see also Refs. [26, 27].
- [26] V. J. Emery and G. Reiter, *Phys. Rev. B* **38**, 4547 (1988); *ibid.* **38**, 11938 (1988).
- [27] J. Zaanen and A. M. Oleś, *Phys. Rev. B* **37**, 9423 (1988).
- [28] These are atomic natural orbital (ANO) basis sets from the MOLCAS library, O $(14s9p)/[4s3p]$ and Cu $(21s15p10d)/[5s4p3d]$, see also Refs. [17, 29].
- [29] R. Pou-Américo, M. Merchán, I. Nebot-Gil, P. O. Widmark, and B. O. Roos, *Theor. Chim. Acta* **92**, 149 (1995).
- [30] P.-Å. Malmqvist and B. O. Roos, *Chem. Phys. Lett.* **155**, 189 (1989).
- [31] For a detailed discussion, see Ref. [7].
- [32] C. L. Kane, P. A. Lee, and N. Read, *Phys. Rev. B* **39**, 6880 (1989).
- [33] K. J. von Szczepanski, P. Horsch, W. Stephan, and M. Ziegler, *Phys. Rev. B* **41**, 2017 (1990).
- [34] E. Dagotto, R. Joynt, A. Moreo, S. Bacci, and E. Gagliano, *Phys. Rev. B* **41**, 9049 (1990).
- [35] P. Fulde, *Electron Correlations in Molecules and Solids* (Springer-Verlag, Berlin, 1995), section 12.6.
- [36] R. Eder and K. W. Becker, *Z. Phys. B* **78**, 219 (1990).
- [37] T. R. Thurston, M. Matsuda, K. Kakurai, K. Yamada, Y. Endoh, R. J. Birgeneau, P. M. Gehring, Y. Hidaka, M. A. Kastner, T. Murakami, and G. Shirane, *Phys. Rev. Lett.* **65**, 263 (1990); B. Keimer, N. Belk, R. J. Birgeneau, A. Cassanho, C. Y. Chen, M. Greven, M. A. Kastner, A. Aharony, Y. Endoh, R. W. Erwin, and G. Shirane, *Phys. Rev. B* **46**, 14034 (1992); M. Greven, R. J. Birgeneau, Y. Endoh, M. A. Kastner, M. Matsuda, and G. Shirane, *Z. Phys. B* **96**, 465 (1995).
- [38] We used effective core potentials for the innermost 12 electrons and the following ANO basis sets from the MOLCAS library for the outer shells of the Zn cations: $(9s6p5d)/[3s2p2d]$, see also Ref. [15].
- [39] T. Tohyama, S. Nagai, Y. Shibata, and S. Maekawa, *Phys. Rev. Lett.* **82**, 4910 (1999).
- [40] J. Miralles, J. P. Daudey, and R. Caballol, *Chem. Phys. Lett.* **198**, 555 (1992); J. Miralles, O. Castell, R. Caballol, and J. P. Malrieu, *Chem. Phys.* **172**, 33 (1993).
- [41] V. M. García, O. Castell, R. Caballol, and J. P. Malrieu, *Chem. Phys. Lett.* **238**, 222 (1995).
- [42] We note that different basis sets were used in Ref. [7].
- [43] C. de Graaf and F. Illas, *Phys. Rev. B* **63**, 014404 (2000).
- [44] E. Bordas, C. de Graaf, R. Caballol, and C. J. Calzado, *Phys. Rev. B* **71**, 045108 (2005).
- [45] A. B. van Oosten, R. Broer, and W. C. Nieuwpoort, *Chem. Phys. Lett.* **257**, 207 (1996).
- [46] C. de Graaf, R. Broer, W. C. Nieuwpoort, and P. S. Bagus, *Chem. Phys. Lett.* **272**, 341 (1997); A. H. de Vries, L. Hozoi, R. Broer, and P. S. Bagus, *Phys. Rev. B* **66**, 035108 (2002).
- [47] J. Zhong and H. B. Schüttler, *Phys. Rev. Lett.* **69**, 1600 (1992).
- [48] A. Ramšak, P. Horsch, and P. Fulde, *Phys. Rev. B* **46**, 14305 (1992).
- [49] A. S. Mishchenko and N. Nagaosa, *Phys. Rev. Lett.* **93**, 036402 (2004).
- [50] P. Prelovšek, R. Zeyher, and P. Horsch, *Phys. Rev. Lett.* **96**, 086402 (2006).
- [51] G. Sangiovanni, O. Gunnarsson, E. Koch, C. Castellani, and M. Capone, *Phys. Rev. Lett.* **97**, 046404 (2006).
- [52] A. Macridin, B. Moritz, M. Jarrell, and T. Maier, *Phys. Rev. Lett.* **97**, 056402 (2006).